Applied Catalysis B: Environmental 223 (2018) 143–153

Contents lists available at ScienceDirect

Applied Catalysis B: Environmental

journal homepage: www.elsevier.com/locate/apcatb

Fe-HFER and Cu-HFER as catalysts for the NO_X SCR using acetylene as a reducing agent: Reaction mechanism revealed by FT-IR *operando* study coupled with ^{15}NO isotopic labelling

Ingrit Castellanos, Olivier Marie*

Normandie Univ, ENSICAEN, UNICAEN, CNRS, Laboratoire Catalyse et Spectrochimie, 14000 Caen, France[1]

ARTICLE INFO

Article history:
Received 28 November 2016
Received in revised form 13 March 2017
Accepted 20 March 2017
Available online 24 March 2017

Keywords:
Acetylene
SCR
Ferrierite
NO_X
Metal cations
FTIR operando
^{15}NO

ABSTRACT

Among NO_X emission sources, the automotive industry and specifically Diesel engines are the main pollutants. Selective catalytic reduction by Hydrocarbons (HC-SCR) may lead to efficiencies as high as 70% in reducing NO_X into N_2 specially by using economical catalysts (zeolites). We report here an HC-SCR study using acetylene (C_2H_2) as a reducing agent that presents intersting activity at low temperatures. A ferrierite zeolite catalyst was used and modified by the introduction of either copper or iron and the NO_X reduction activity was analysed by InfraRed (IR) *operando* techniques subsequent to a preliminary *IR in-situ* characterization. The later technique allowed the identification of the species formed on the surface after NO or C_2H_2 adsorption at room temperature. The thermal stability of adsorbed acetylene was also investigated. The obtained information on vibrational bands typical for adsorbed species served as an input for the IR *operando* study. Cu-HFER catalyst presents a strong redox character upon room temperature interaction with NO as well as a strong affinity for C_2H_2 adsorption. However, Fe-HFER shows a higher NO_X reduction efficiency when submitted to SCR conditions. Indeed, iron ions enhance the NO oxidation into NO_2 that seems to be more reactive with C_2H_2. The reaction mechanism was revealed by an FT-IR *operando* study coupled with ^{15}NO isotopic labelling that proved the formation of hydrocyanic acid and isocyanate species as key intermediate species.

1. Introduction

The abatement of nitric oxides ($DeNO_X$) from Diesel exhausts is a controversial topic. Two years after the implementation of EURO 6 directives, the efforts for automotive companies to meet the NO_X emission level in Diesel engines remains quite strong. The world's present average NO_X emissions are seven times higher than the Euro emission limit (0.6 g/km vs. 0.08 g/km) [1]. In particular, heavy duty Diesel engine manufacturers demand effective $DeNO_X$ processes. Commercial selective catalytic reduction (SCR) systems actually use ammonia as reducing agent. However, such a reducing agent presents some limitations due possible slips of this corrosive gas, a rather low efficiency below 250 °C and toxicity of typically used catalysts ($V_2O_5/WO_3/TiO_2$). Results from Iwamoto et al. [2] point hydrocarbons as a promising alternative to ammonia. Interest for hydrocarbons rely on the use of zeolites as economic catalysts. Recent studies compared the activity of different kinds of hydrocarbons, such as ethene (C_2H_4), propene (C_3H_6), propane (C_3H_8) and butene (C_4H_8). Acetylene (C_2H_2) as a reducing agent also presents reasonable efficiencies to reduce NO_X [3] together with almost no diffusional limitation in the intracrystalline porous system of zeolite catalysts [4]. Moreover, acetylene could be generated in situ over calcium carbide [$CaC_2 + 2H_2O \rightarrow C_2H_2 + Ca(OH)_2$] representing an advantage for its on-boarding (related to security), dosing (gas injection instead of liquid urea solution) and application.

Concerning the zeolitic catalysts, pentasil zeolites (ZSM-5, FER...) have shown higher NO_X conversions than sodalite type zeolites (A, Y, SAPO...) since the NO to NO_2 oxidation seems to be improved [5]. Moreover, transition metal ions (TMI) introduced in the zeolite catalyst show the best performances for the above mentioned NO oxidation. In fact, due to the redox properties of TMI, several reactions can be carried out at the active sites of the catalyst, enhancing the selectivity towards N_2 during HC-SCR conditions.

This work will deal with the study of the SCR of NOx using C_2H_2 as a reducing agent over Ferrierite catalysts loaded with two different ions: iron and copper. The choice of the FER structure was

* Corresponding author.
E-mail address: olivier.marie@ensicaen.fr (O. Marie).
[1] 'Permanent address' for the second author and 'Present address' for the first author.

http://dx.doi.org/10.1016/j.apcatb.2017.03.052
0926-3373/

Table 1
Elemental composition of our zeolites from ICP-AES analysis.

Sample	Si/Al ratio	Metal wt.%	M/Al ratio
1%Fe–HFER	8.84	0.73	0.09
1%Cu–HFER	8.86	0.88	0.10

guided by its efficiency in SCR with small chain hydrocarbons [6]. Prior to the catalytic tests operated in the *IR operando* mode, the redox properties of the surface will be analysed by adsorption of probe molecule followed by *in-situ* FT-IR spectroscopy. Firstly, the NO adsorption at room temperature will allow the identification of typical bands formed when the catalyst is pretreated under oxidizing or reducing atmosphere. Secondly, the study of C_2H_2 adsorption will give novel information about its interaction with TMI along with its thermal stability. Finally, the behaviour of the catalyst during SCR conditions will be investigated by *operando* FT-IR spectroscopy. Applying such a powerful methodology, the gas phase activity measurement and the nature of intermediate species can be evaluated simultaneously under working conditions. Coupled with the use of isotopically labelled ^{15}NO molecule, the *IR operando* results will allow the determination of the reaction mechanism.

2. Experimental part

2.1. Catalyst preparation

The mother zeolite used in this work presents a specific surface $S_{BET} = 170\ m^2\ g^{-1}$. It was obtained from TOSOH Company (HSZ-700 series, FERRIERITE). A solution of NH_4Cl (0.1 M) was prepared in order to exchange K and Na ions by NH_4^+. Total exchange was carried out by repeating three times the suspension of mother zeolite in the ammonium aqueous solution at 80 °C under stirring during 3 h. After each exchange step, the catalyst was centrifuged twice for 10 min and three times for the last exchange. Finally, the recovered catalyst was dried at 100 °C for 12 h. Two aqueous solutions containing the Transition Metal Ion (TMI) target at 10^{-3} M concentration were then prepared: iron sulphate ($FeSO_4$) for the introduction of iron ions and copper acetate ($Cu(CH_3COO)_2$) for copper ions (purchased from Sigma-Aldrich). The ion exchange was performed under stirring during 4 h at 80 °C. This metal cation introduction was repeated twice, the suspension obtained after the first exchange being submitted to centrifugation before the next one.

For each experiment, the catalyst was pressed into self-supported wafers (diameter = 16 mm and thickness ≈30 mm) and heated at 450 °C for 2 h (heating rate of 2 °C min^{-1}) without any preliminary calcination.

The two samples are further called 1%Fe–HFER and 1%Cu–HFER according to elemental analysis data summarized in Table 1 and Fig. SI.1 shows the XRD profiles of these catalysts.

2.2. *IR* in-situ *adsorption tests*

The redox properties of the catalysts were studied by the *in-situ* IR method using nitric oxide (99.908% NO, AIR-LIQUID) as a suitable probe molecule being also one reactant of the SCR process. Prior to NO adsorption, two different pre-treatments were performed on the sample located in the *in-situ* IR cell. At the end of the heating period up to 450 °C under a vacuum, the first pre-treatment consists in the introduction of 1.33×10^4 Pa of oxygen (100% O_2–ALPHAGAZ 1 Oxygen, AIR-LIQUIDE) in the *in-situ* IR cell for 30 min. The sample is then cooled down at 200 °C at which oxygen is removed under dynamic vacuum. For the second pre-treatment, hydrogen (99.999% H_2–ALPHAGAZ 2 Hydrogen, AIR-LIQUIDE) is used and introduced in a similar way (identical temperature, pressure and residence time). H_2 removal is however performed at 450 °C under dynamic vacuum. Regarding the acetylene adsorption (99.6998% C_2H_2, AIR LIQUIDE), a fresh catalyst is used and heated up to 450 °C under a vacuum (<10^{-4} Pa) before its adsorption at room temperature. For the NO or C_2H_2 adsorption, small doses between 14–237 $mmol/g_{catalyst}$ are introduced over each sample. Increasing equilibrium pressures (133, 266, 532, 666, 1067 and 1333 Pa) of probe molecule are then introduced in contact with each catalyst.

Aiming at testing the thermal stability of adsorbed C_2H_2, a temperature programmed desorption (TPD) was finally performed by 50 °C increments from room temperature up to 300 °C.

A Nicolet 6700 FTIR spectrometer equipped with a DTGS detector was used to record the IR spectra at a spectral resolution of 4 cm^{-1} and an accumulation of 128 scans.

2.3. *IR* operando *tests*

Concerning the catalytic tests, the IR *operando* methodology was applied. More details about the IR cell-reactor and the experimental set-up are available in [7,8]. The pre-treatment of the sample was performed under a flow of 10% O_2 in Ar at 450 °C during 2 h with a heating rate of 2 °C min^{-1}. Prior to starting the reaction, the temperature was decreased down to 100 °C. The Temperature Programmed Surface Reaction (TPSR) study of the catalyst activity was then performed between 100 and 450 °C at a 2 °C.min^{-1} heating rate. The reaction flow made of 400 ppm ^{14}NO (or ^{15}NO), 10% O_2 and 200 ppm C_2H_2 in Ar was established by mass flow controllers and its stability checked by Mass Spectrometry (Quadrupole Pfeiffer Omnistar GSD 301) before switching to the IR cell for catalytic reaction. A space velocity of 100 L h^{-1} g^{-1} was used.

The analysis of the gas at the outlet of the IR reactor cell was achieved simultaneously by Chemiluminescence (Thermo-Scientific, model 42 *i*-HL) and IR spectroscopy (Thermo Nicolet NEXUS 670 FTIR equipped with a MCT detector) techniques. The former measures the NO and NO_2 concentrations while the latter provides the C_2H_2, N_2O and CO concentrations. The analysis of the species adsorbed at the catalyst's surface under operating conditions was performed by IR spectroscopy. The spectra for both the gas phase and the adsorbed species were recorded with a spectral resolution of 4 cm^{-1} (64 scans).

3. Results and discussion

Table 1 reports the main characteristics relative to catalysts composition. A preliminary step required before studying the catalysts under duty consists in the characterization of their superficial properties. The Fe-HFER sample has already widely been characterized by CO and NO adsorption followed by IR spectroscopy and complementary Mossbauer spectroscopy [8–10], however the Cu-HFER involved in the present work requires the characterization of its Cu redox centres, as possible active sites.

3.1. Identification of Cu^{X+} (x = 1, 2 or 3) species by NO adsorption

Fig. 1 presents the *in-situ* IR spectra of NO adsorption over Cu–HFER after two different pre-treatments (O_2 and H_2). The nature of the pretreatment affects in a noticeable way the observed IR vibrations indicating a high sensibility of the copper to a reducing or an oxidizing atmosphere. The assignment of most of the detected bands is based on previous studies performed over different zeolitic structures [11]. After the reducing pretreatment (H_2), a remarkable intensity of the band at 1808 cm^{-1} corresponding to NO adsorption over Cu^+ ions is detected. On the contrary, after the oxidizing pretreatment (O_2) this band possesses a very low intensity, while other bands at 1905 and 1914 cm^{-1} become very strong. These two last

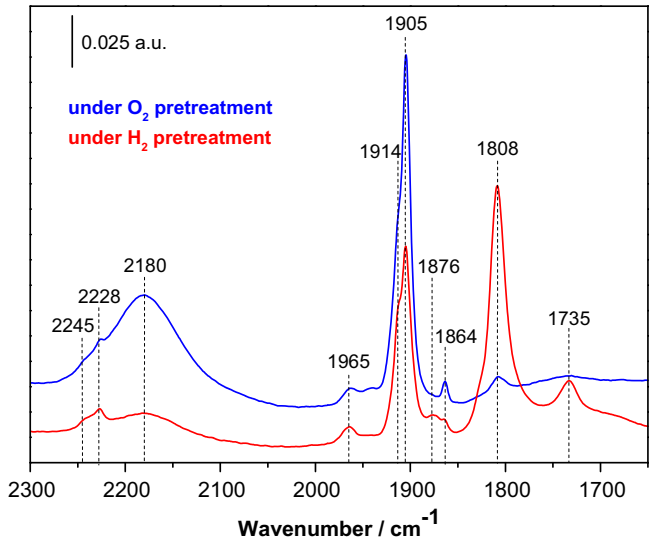

Fig. 1. IR spectra obtained for 1%Cu–HFER under a NO equilibrium pressure of 1067 Pa after pretreatment at 450 °C during 2 h under O_2 (upper, blue spectrum) or H_2 (lower, red spectrum) and cooling down to 25 °C prior to spectra recording. All the spectra are corrected with the reference spectra recorded prior to NO adsorption.

bands are identified as characterizing two distinct Cu^{2+} mononitrosyls even if they are also observed after the reducing pretreatment. The previous observations thus indicate the simultaneous presence of Cu^{2+} and Cu^{+} ions in the FER zeolite whatever the pretreatment. After the oxidizing one, the scarce presence of mononitrosyls on Cu^{+} ions is tentatively explained by the favored oxidation of isolated but very close Cu^{+} cations to Cu^{2+} by O_2, according to Eq. (1).

$$2Cu^{+} + ½O_2 \rightarrow Cu^{2+} - O^{2-} - Cu^{2+} \quad (1)$$

The copper dimeric species $[Cu^{2+} - O^{2-} - Cu^{2+}]$ have indeed been identified in previous works [12].

The detection of Cu^{+} ions during the NO addition after an oxidizing pretreatment may then appear surprising given the expected greater stability of Cu^{2+} ions. It is suggested that the *in-situ* formation of Cu^{+} ions would be associated with the reduction of Cu^{2+} involving the NO^{+} formation (band at 2180 cm^{-1}) following Eqs. (2) and (3).

$$Cu^{2+} - O^{2-} - Cu^{2+} + NO \rightarrow Cu^{2+} - O^{2-}...NO^{+} + Cu^{+} \quad (2)$$

$$Cu^{2+} - O^{2-}...NO^{+} \rightarrow Cu^{+} + NO_2 \quad (3)$$

In agreement with this hypothesis, the intensity of the NO^{+} band at 2180 cm^{-1} [13] is higher after the oxidizing pretreatment. NO thus plays the role of a reducing agent when the sample has been preoxidized.

On another hand, after a pretreatment under H_2, the significant intensity of the bands at 1905 and 1914 cm^{-1} indicates that Cu^{2+} mononitrosyls are still quite present in the Cu–HFER sample after such a reducing pretreament. Indeed, the Eq. (4) proposes the Cu^{+} oxidation upon interaction with NO leading to the formation of N_2O (bands at 2228 and 2245 cm^{-1}).

$$2Cu^{+} + 2NO \rightarrow Cu^{2+} - O^{2-} - Cu^{2+} + N_2O \quad (4)$$

In agreement with this hypothesis, the intensity of the N_2O is higher after a reducing pretreatment. NO thus acts as an oxidizing agent when the sample has been prereduced.

In addition, after the reducing pretreatment, few dinitrosyls species $[Cu^{+}(NO)_2]$ are evidenced by their asymmetric and symmetric vibration bands at 1735 and 1828 cm^{-1}, respectively. The later band is detected as a shoulder at the 1808 cm^{-1} band. The band at 1876 cm^{-1} represents the interaction of NO with the Brønsted acidic sites [–OH] of the FER as observed for the sample without TMI (spectra not reported here). The nature of the band at 1864 cm^{-1} is still unclear.

Concerning the band at 1965 cm^{-1} present for both pretreatments, a recent study proposes the formation of Cu^{3+} mononitrosyls in Cu-ZSM-5 [14] leading to a n(NO) at a similar wavenumber. Although this copper oxidation degree is not commonly observed, such a high wavenumber is consistent with this hypothesis. After the reducing pretreatment, the formation of Cu^{3+} ions would result from the dismutation reaction induced by NO adsorption on the copper dimeric species according to Eq. (5).

$$Cu^{2+} - O^{2-} - Cu^{2+} + 2NO \rightarrow Cu^{3+} = O^{2-}...NO + Cu^{+}...NO \quad (5)$$

3.2. C_2H_2 interaction with Fe^{x+} and Cu^{x+} ions

This section focuses on the C_2H_2 interaction with iron and cupper cations: its adsorption at room temperature and its thermal desorption. As mentioned elsewhere [8], the C_2H_2 adsorption leads to the formation of different bonds depending on the nature of the interacting site. A hydrogen bond is established with Brønsted acids (–OH) while a m-p-bonding is established with Lewis acids (M^{X+}) [15]. Both types of bonding lead to a red-shift of the n_{as}(CH) compared to the gas phase one (3282 cm^{-1}). Indeed, the partial overlapping of s type orbital of a given cation (H^{+} or M^{X+}) with the C_2H_2 p bonding orbital provokes a lowering of the electron density in the inter-nuclear region thus leading to a lowering of the CC bond order. In a similar way, an increase of the charge density in the C_2H_2 p anti-bonding orbital through overlapping with the populated 3d orbitals of transition metal leads to a lowering of the CC bond order [15,16]. As a consequence the n(CH) together with the n(CC) vibrations are submitted to a red-shift.

Fig. 2 shows the evolution of the infrared bands upon increasing small amounts of C_2H_2 interacting with 1%Fe–HFER (upper part) and 1%Cu–HFER (bottom part). The C_2H_2 adsorption was previously performed on the acidic form of the catalysts (HFER) in order to identify the band related to the interaction with the Brønsted sites and further distinguish them from those associated to the C_2H_2 interacting with Lewis sites (Fe or Cu ions) [8]. Hence, the band detected here at 3223 cm^{-1} and common for both catalysts represents the n_{as}(CH) of C_2H_2 interacting with Brønsted acids (–OH). The broad band at 3385 cm^{-1} increasing in parallel with that at 3223 cm^{-1} characterizes the hydroxyl groups $n(OH)_P$ perturbed by Hydrogen bonding as previously mentioned by Bordiga et al. [16].

As a consequence, the two main bands assigned to n_{as}(CH) of acetylene adsorbed on Fe^{2+} and Cu^{+} ions (most abundant species after a reducing pretreatment) are those at 3183 and 3175 cm^{-1}, respectively. The 8 cm^{-1} difference between these bands indicates a stronger interaction of C_2H_2 with copper ions than with iron ions.

In the case of 1%Fe–HFER and 1%Cu–HFER, smalls band at 3270 and 3246 cm^{-1} respectively increase in parallel with those at 3183 and 3175 cm^{-1}, respectively, but a complementary analysis of the bands detected in the n(CC) low wavenumbers range is necessary to explain their nature.

For both catalysts, three common bands are present in the above mentioned n(CC) range at about 1949-1946 (shift), 1954 and 1957 cm^{-1}. The rising of two later bands is correlated with the increase of the band at 3223 cm^{-1}. They thus represent the n_s(CC) of C_2H_2 interacting with Brønsted acids (–OH). Multiple bands are observed for the n_s(CC) while only one is observed for the n_{as}(CH), the former being thus more sensitive than the later to the heterogeneity of the hydroxyl acidic groups (Al-OH-Si). The 1946 (1949) band that evolves at first would characterize the presence of traces of Al^{3+} Lewis acids.

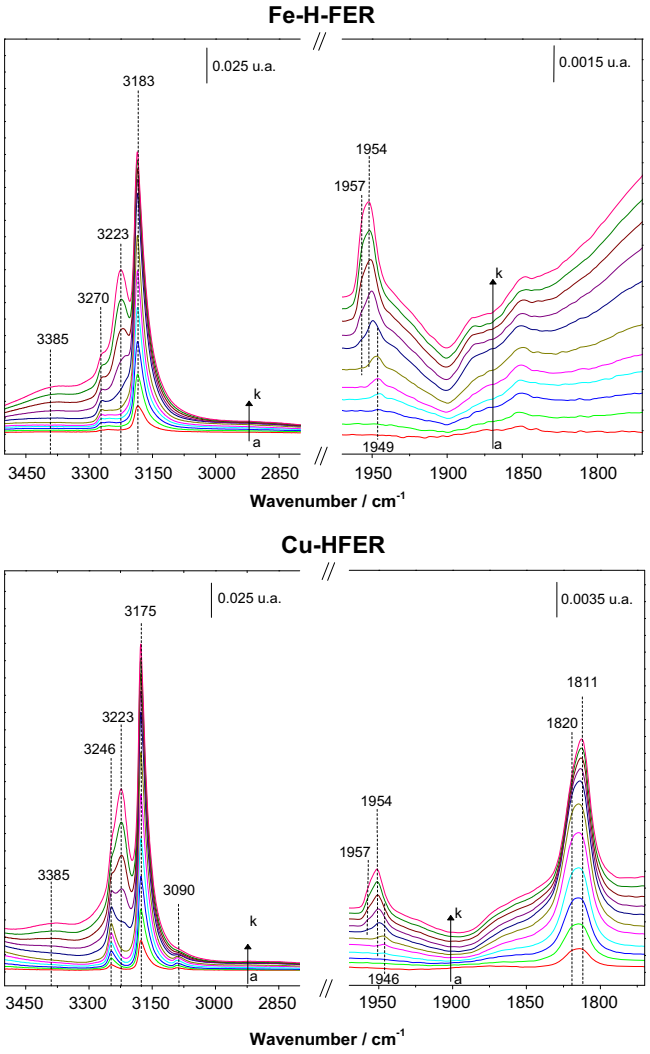

Fig. 2. IR spectra obtained for C_2H_2 adsorption at low concentration between 14 and 237 mmolg^{-1} over Fe–HFER (upper part) and Cu–HFER (bottom part). The samples were activated at 450 °C during 2 h under vacuum and cooled down to 25 °C prior to spectra recording. All the spectra are corrected with the reference spectra recorded prior to C_2H_2 adsorption.

Concerning the n_s(CC) of C_2H_2 interacting with the loaded transition metal cations, no well defined band was observed for the interaction between C_2H_2 and Fe^{2+} ions because of the geometry of the adsorption mode, as previously reported [8]. In contrast, with the 1%Cu–HFER catalyst, the apparition of two n_s(CC) bands is observed from the very first doses. The rising of these bands at 1811 and 1820 cm^{-1} is concomitant with the rise of those at 3246 and 3175 cm^{-1} [n_{as}(CH) of C_2H_2 on Cu^+ ions]. The pair of bands at 1811 and 1820 cm^{-1} thus characterizes the interaction of C_2H_2 with Cu^+ ions. Such a wavenumber is quite low when compared with that observed for acetylene interacting with Co–HFER (1925 cm^{-1}) for example [8] and traduces a very high lowering of the (CC) bon order. Recent DFT studies have considered the possible formation of a bridged bonding between the C_2H_2 and dual Cu^+ species [17]. Such a kind of interaction could take place in our present case given the proximity of Cu^+ ions observed during the NO adsorption: the formation of the copper dimeric species [$Cu^{2+} - O^{2-} - Cu^{2+}$] was indeed detected. Moreover, such a bridging acetylene species would explain the shift of the n(CC) band by a consequent lowering of the CC bond order upon simultaneous interaction with two Cu^+ ions. An alternative/complementary explanation for the high n(CC) red shift compared to cobalt ions lies in the stronger p-retro-donation from $3d^{10}$ for Cu^+ compared to $3d^7$ for Co^{2+}. One points however remains not clear: if the 3246 and 3175 cm^{-1} bands together with those at 1811 and 1820 cm^{-1} characterize the interaction of acetylene with Cu^+ entities, why such a big shift is observed in the n_{as}(CH) range while it was identified as less sensitive that the n(CC) range in the case of an interaction with the hydroxyl groups?

It should be here reminded that the n_{as}(CH) of C_2H_2 in the gas phase is split as a result of a Fermi resonance between the fundamental n_3 mode and the ($n_2 + n_4 + n_5$) combination one (notation from [18]). Upon adsorption, such a spectroscopic phenomenon usually disappears since, generally speaking, each vibration mode shifts in a different way and the match for Fermi resonance does not exist anymore. However, in the present case of Cu–HFER, both the n_3 [n_{as}(CH)] and n_2 [n_s(CC)] shift in similar way: (3289 → 3175) and (1974 → 1820/11) respectively. It is suggested that Fermi resonance would occur generating a spectroscopic splitting of the n_{as}(CH) in two bands at 3246 and 3175 cm^{-1}. This in turn means that these two resulting bands do not represent two distinct chemical species even if the n(CC) split indicates that C_2H_2 interact with two distinct Cu^+ sites! Such a Fermi resonance would also be observed for the C_2H_2 adsorbed on the Fe containing catalysts and would explain the shoulder observed at 3270 cm^{-1}.

Finally, revisiting the high wavenumbers range, a low intensity band at 3090 cm^{-1} is found to be present from the beginning of the C_2H_2 adsorption on copper ions. Such a band is not observed on Cu-zeolites where Brønsted acidity is absent [17]. However, Cremer et al. [19] reported the formation of m-vinylidene (Pt = C=CH_2) species on Pt (111) at similar wavenumbers (3030 cm^{-1}). We propose that the proximity between protons and copper ions in our sample, together with a strong decrease in the order of the CC bond, allows the formation of similar vinylidene species in Cu–HFER.

The thermal stability of species formed during C_2H_2 adsorption over the two catalysts was also considered. This will provide relevant information about the nature of the species formed during the catalyzed reduction of nitrogen oxides. Fig. 3 shows the spectra recorded every 50 °C during the rising ramp of temperature under a dynamic vacuum ($P < 10^{-4}$ Pa). After the room temperature evacuation of C_2H_2, both catalysts still exhibit the bands described above. It is recalled that they are assigned to the n_{as}(CH) of C_2H_2 on iron cations (Fig. 3A, band at 3185 cm^{-1}) and copper cations (Fig. 3B, bands at 3246, 3177, 3090 cm^{-1}). No band typical for the 'soft' interaction between C_2H_2 and Brønsted acids (–OH) remained. However, the thermal activation of hydrogen transfer leading to C_2H_2 protonation cannot be excluded during further temperature increase. The resulting bands, present at 3131 cm^{-1} observed with Cu–HFER would represent another kind of species: the polyenes (as reported in [16]) arising from acetylene oligomerization.

Focusing in the n_{as}(CH) of C_2H_2, it is observed that the thermal stability of C_2H_2 interacting with TMI depends on the cation: at about 100–150 °C for iron ions and 200–250 °C for copper ions. The interaction between the C_2H_2 and Cu^+ ions is thus confirmed as the strongest one.

3.3. Acetylene and nitric oxide oxidation

Comparing the reducing agent consumption in NO SCR conditions or in combustion conditions ($C_2H_2 + O_2$) clearly indicates the faster conversion of C_2H_2 when NO_X are present in the flow (see Figure SI.2.). However, aiming at better understanding the involvement of C_2H_2 in NO_X reduction, it is first important to characterize the individual interaction of both C_2H_2 and NO with O_2. Indeed, two oxidation reactions are present when dealing with the deNO_X by hydrocarbons: the oxidation of the reducing agent and that of NO. Here, information concerning the limits of these reactions, each

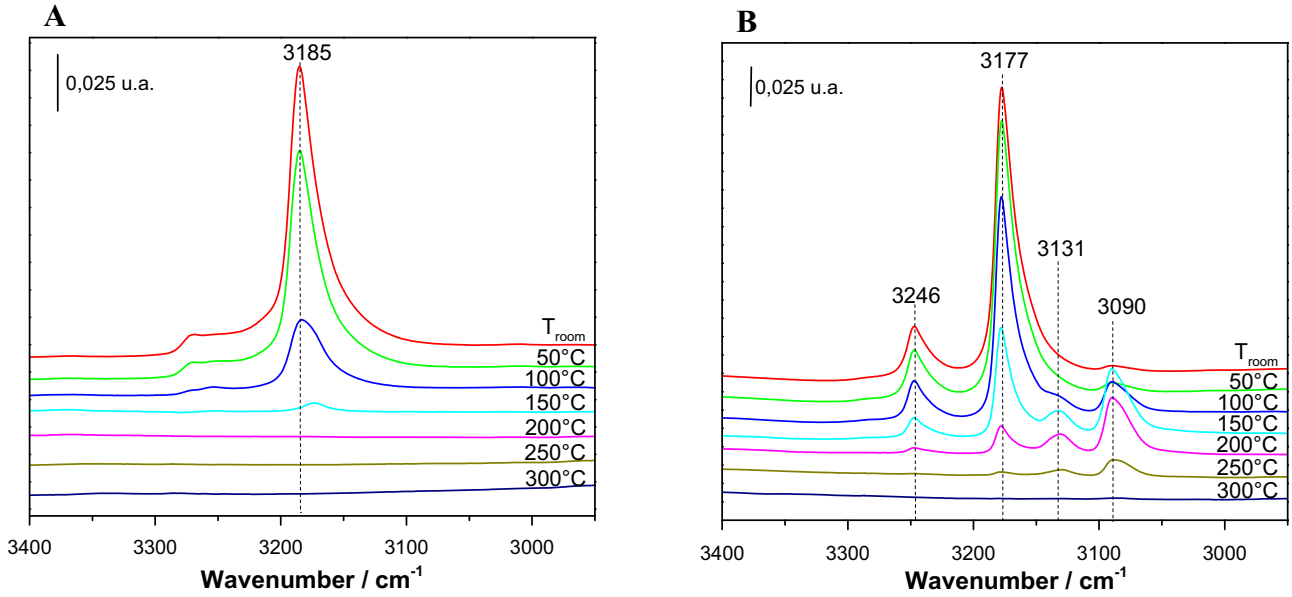

Fig. 3. IR spectra recorded during thermal desorption every 50 °C under a dynamic vacuum (P < 10^{-4} Pa) on: A) 1%Fe–HFER and B) 1%Cu–HFER catalysts.

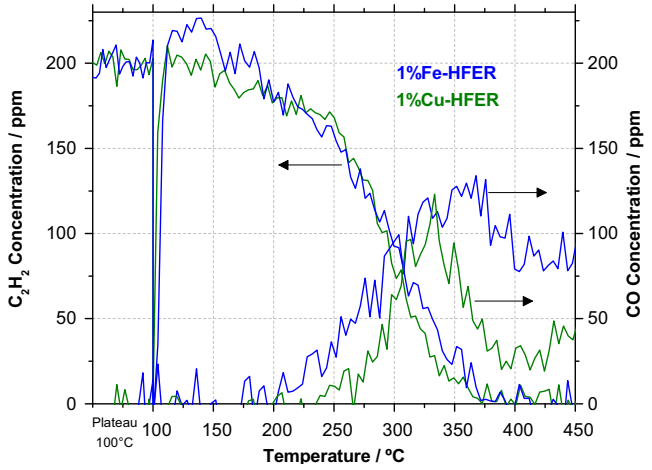

Fig. 4. Evolution of the C_2H_2 concentration during its oxidation over 1%Fe and 1%Cu –HFER catalysts together with the evolution of the CO production. Test conditions: 200 ppm C_2H_2; 2.5% O_2; SV: 100 L h^{-1} g^{-1}.

considered separately, are investigated before submitting the catalysts to the proper HC-SCR conditions. Figs. 4 and 5 respectively show the evolution of the C_2H_2 and NO at the outlet of the IR-cell reactor. As observed in Fig. 4, little difference is detected concerning the C_2H_2 conversion over both catalysts. Under our operating conditions, the catalysts activity for this reaction starts at about 175 °C, reaching a total conversion at 400 °C. The light off temperature (defined at 50% of conversion) is measured at $T_{L.O.}$ = 300 °C. Regarding the product distribution, a rather high amount of CO (about 125 ppm at 350 °C) is detected with the iron containing sample while the full oxidation to CO_2 is favored over the Cu–HFER in the high temperature range. This may arise from higher adsorption strength of C_2H_2 over Cu cations (as revealed from the *in situ* part) thus keeping it more available on the active site for complete oxidation to CO_2.

The wide temperature range for acetylene activation especially in the low temperature region should be optimal for NO_X removal by C_2H_2. Indeed, it is known that the HC-SCR efficiency is often limited at low temperatures. For example, with CH_4 temperatures as high as 300 °C are necessary to break the C—H bond and form active species needed in the NO_X reduction [20].

As a conclusion, it is worth reminding that difference between both catalysts under C_2H_2 oxidation working conditions is only detected in the products distribution being more selective the 1%Cu–HFER catalyst towards CO_2 most probably related to its high affinity with C_2H_2 compared to the 1%Fe–HFER catalyst.

A completely different behaviour is observed when considering the NO oxidation. In the low temperature region (100 < T < 135 °C), Fig. 5A shows a more pronounced NO_X adsorption over 1%Fe–HFER compared to 1%Cu–HFER (Fig. 5B). Then, upon increasing temperature, the 1%Fe–HFER sample reaches a NO to NO_2 conversion as high as 65% between 300 and 320 °C. On the contrary, the maximal NO conversion over 1%Cu–HFER only reaches about 25% at 450 °C. The iron-containing sample thus provides a much higher NO oxidation activity. It is worth noting that N_2O was not detected during these NO to NO_2 oxidation experiments.

These results are quite surprising for the copper-containing sample, given the Cu^{x+} redox behaviour evidenced during the NO adsorption tests performed after different pre-treatments. Several parameters have been previously reported to affect the NO to NO_2 efficiency, among them the P_{O2}/P_{NO} ratio, the kind of zeolite structure and the copper degree of exchange [2]. In our present case, the P_{O2}/P_{NO} is already quite high and the thermodynamic concentration of NO_2 at equilibrium under those conditions is reported in Fig. 5A and B to provide evidence that NO_2 formation for both catalysts is kinetically governed. Furthermore, dealing with the zeolite framework and TMI loading, the FER structure is efficient when iron loaded and the Cu exchange degree is similar to the iron one. The poor NO to NO_2 efficiency for the Cu–HFER thus remains unexplained and according to the above results it should be concluded that under our working condiditons, copper dimers species [Cu^{2+}-O^{2-}-Cu^{2+}] are more reactive towards C_2H_2 than towards NO.

In summary, the iron hosted in the HFER shows efficient activity for both C_2H_2 and NO oxidation reactions compared to the copper-containing zeolite that only presents high C_2H_2 conversion levels. This Fe–HFER behaviour is desired when acetylene is used as reducing agent in NO_X reduction, especially for the NO oxidation to NO_2 which is supposed as the major rate determining step [8].

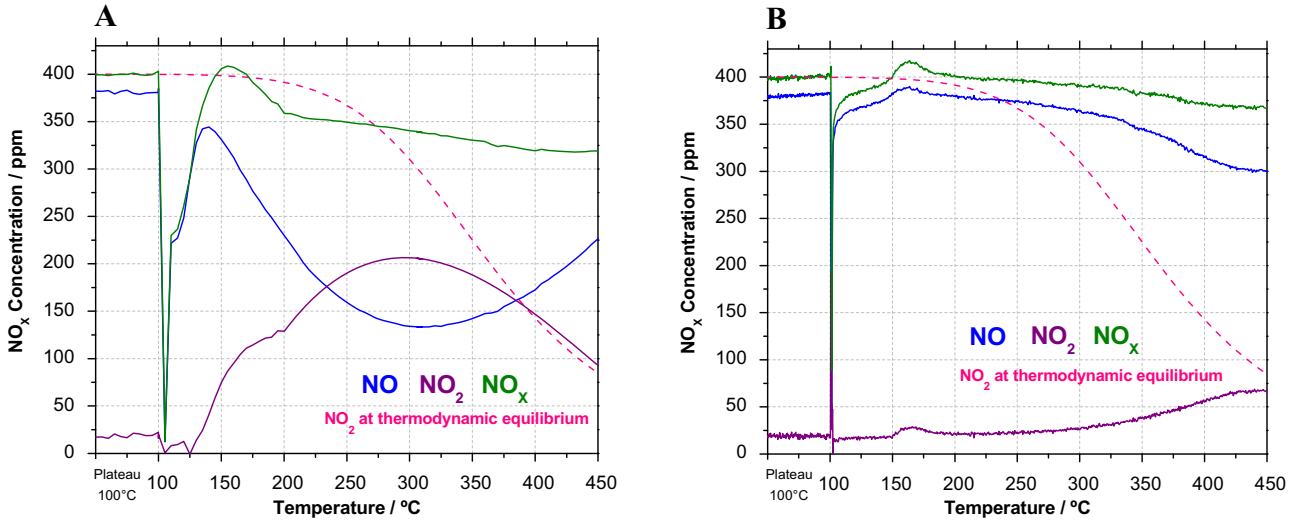

Fig. 5. Evolution of the NO, NO_2 and NO_x concentration during NO oxidation over: A) 1%Fe–HFER and B) 1%Cu–HFER catalysts. Test conditions: 380 ppm NO; 2.5% O_2; SV: 100 L h^{-1} g^{-1}.

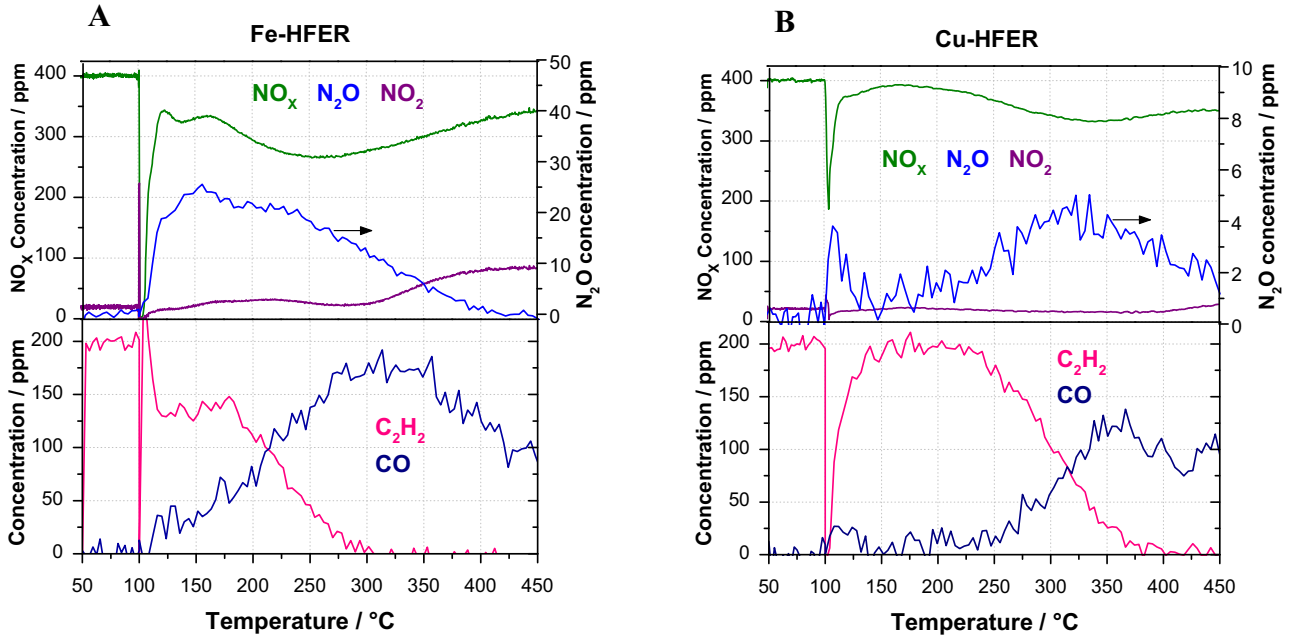

Fig. 6. Evolution of the NO_X, NO_2, N_2O, C_2H_2 and CO for: A) 1%Fe–HFER and B) 1%Cu–HFER catalysts. Test conditions: 400 ppm NO; 200 ppm C_2H_2; 2.5% O_2; SV: 100 L h^{-1} g^{-1}.

3.4. NO_X C_2H_2-SCR: a gas phase approach

The deNO_X activity was evaluated under pure NO conditions (400 ppm) and the evolutions of C_2H_2, CO, NO_X, NO_2, N_2O concentrations are shown for Fe–HFER in Fig. 6A and for Cu–HFER in Fig. 6B. The plots start from 150 °C since only adsorption onto the catalyst is observed for both samples between 100 and 150 °C.

Regarding the total NO_X concentration (Fig. 6A and B), an obvious higher NOx removal efficiency is detected when 1%Fe–HFER is used compared to 1%Cu–HFER. At 150 °C, the former reaches a NO_X conversion around 20% while the later does not present any activity. However, the Fig. 6A clearly illustrates that in this low temperature range, the selectivity towards N_2O is rather high.

When the temperature increases, the NO_X conversion over the 1%Fe–HFER sample reaches a maximum of 34% at 260 °C, while for the 1%Cu–HFER sample the maximal NO_X conversion only reaches 17% at 330 °C.

As observed in Fig. 6, the total NO_X concentration is correlated, in the low temperature range [125–175 °C], with the C_2H_2 evolution: particularly for Fe–HFER a higher acetylene conversion than that detected during the preliminary oxidation test clearly reveals its participation in the NO_X reduction. The higher SCR efficiency of the 1%Fe–HFER catalysts is thus related with its acetylene $T_{L.O.}$ = 210 °C compared to $T_{L.O.}$ = 300 °C for 1%Cu–HFER. Moreover, the analysis of the CO production reveals for Fe–HFER a higher amount of CO production in SCR conditions than in C_2H_2 combustion conditions (Fig. 4). This indicates that CO is a by-product from SCR reaction that Fe–HFER is not able to convert to CO_2 as evidenced by the already high amount of CO observed in combustion conditions compared with that measured over the Cu–HFER catalyst.

On another hand, the full C_2H_2 conversion being reached at 300 °C with the 1%Fe–HFER catalyst, a decrease of the deNO_X activity is observed as a consequence of this lack of reducing agent (Fig. 6A).

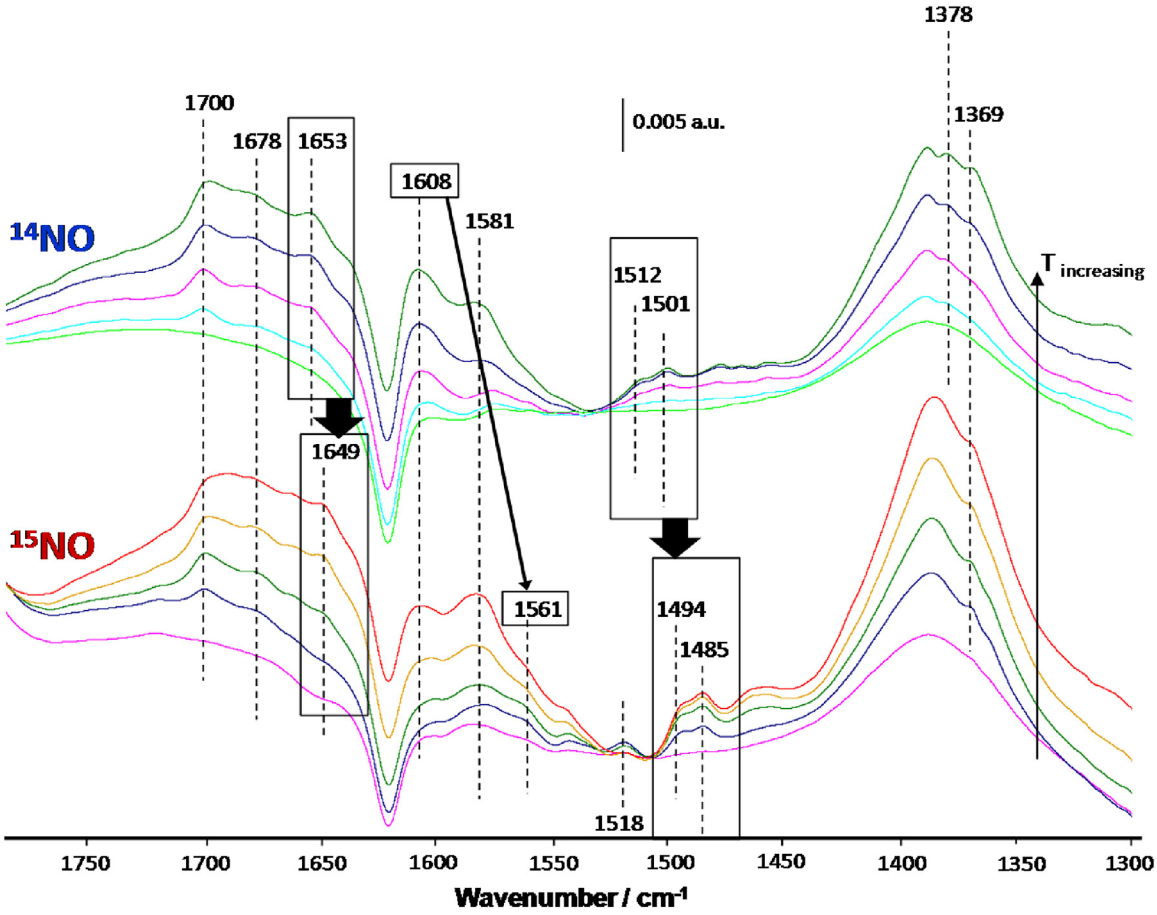

Fig. 7. IR spectra recorded between 104 and 120 °C for 1%Fe–HFER catalyst submitted to NO-SCR catalytic test. Conditions: 400 ppm ^{14}NO (upper series) or ^{15}NO (lower series); 200 ppm C_2H_2; 2.5% O_2; SV: 100 L h^{-1} g^{-1}. Spectra collected every 4 °C.

In summary, the involvement of C_2H_2 in the low temperature reduction of NO_X is clearly revealed but when C_2H_2 becomes fully converted at higher temperatures, its consumption through direct combustion increases thus leading to a decrease of NO_X removal. Indeed, C_2H_2 does not react exclusively with the NO_X since the presence of O_2 also leads to its combustion.

3.5. 1%Fe–HFER catalyst: mechanism revealed by isotopic $^{14}NO/^{15}NO$ labelled

The investigation of intermediate species formation at the catalytic surface during the deNO_X reaction will now be performed. The study will be achieved with the iron-containing sample, given the higher performance of this catalyst under pure NO SCR conditions.

The use of ^{15}NO labelled isotope under SCR conditions is of primary importance to allow the identification of infrared bands corresponding to nitrogen-containing intermediate species. This will greatly help to assess new bands assignments.

Figs. 7–10 show the IR spectra recorded at different temperatures for both labelled and non-labelled work conditions (performed separately): 400 ppm ^{14}NO or 400 ppm ^{15}NO. In the lower temperature range (Fig. 7), i.e when mostly adsorption takes place, some shifts are already observed and identification of nitrogen-containing species is possible. Table 2 summarizes the isotopic shift factors for $^{15}N—O$ or $C—^{15}N$ vibrations calculated from the reduced masses of harmonic diatomic vibrators. These estimated values will be useful for the identication of chemical bonds involving nitrogen.

Table 2
Isotopic shift factors for N—O and C—N harmonic vibrators.

^{14}N	^{15}N	ν_i/ν
$^{14}N—O$	$^{15}N—O$	0.9820
$C—^{14}N$	$C—^{15}N$	0.9845

Bands detected at 1501, 1512, 1608 and 1653 cm^{-1} when using ^{14}NO all shift towards lower wavenumbers when using ^{15}NO (Fig. 7). One obtains the following isotopic shift factors: 0.9881 for the bands at 1501 and 1512 cm^{-1}; 0.9708 for the band at 1608 cm^{-1} and 0.9976 for the band at 1653 cm^{-1}. The set of three bands at 1501, 1512 and 1653 cm^{-1} thus displays quite higher shift factors than those reported in Table 2. A careful analysis of literature data indicates that the comparison with estimated value in Table 2 is helpful but not sufficient since the split of the N—O modes to symmetric and antisymmetric also affects the isotopic shift, being broad the range [0.9759–0.9938] of reported isotopic factors for $^{14}N—O \rightarrow {}^{15}N—O$ bonds of species formed over ZrO_2 based catalyst [21]. However, the comparison of isotopic factors should be made for comparable initial band position. Indeed, for the degenerated n_3 mode of nitrates, the highest reported isotopic shift factor of 0.9938 corresponds to the n_3" vibration (low frequency band) of bridged nitrates species characterized by an IR band initially at 1235 cm^{-1}. The same work reports that the highest observed isotopic shift for the $n_3¢$ vibration (high frequency band) is 0.9796. These data thus confirm that isotopic factor as high as 0.9881 (detected in our work) was not reported for band initially located at about 1500 cm^{-1} (detected in our work) and that would involve a NO vibration.

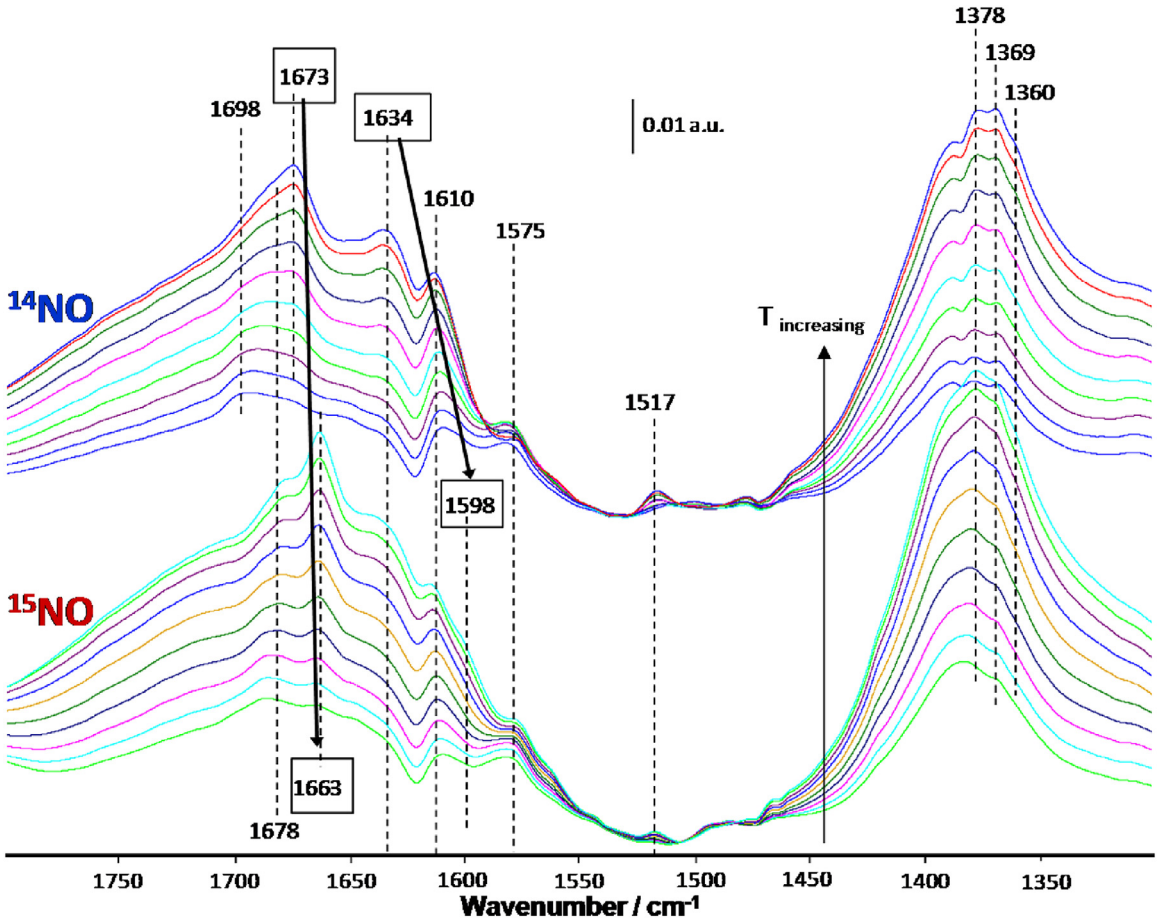

Fig. 8. IR spectra recorded between 120 and 160 °C for 1%Fe–HFER catalyst submitted to NO-SCR catalytic test. Conditions: 400 ppm ^{14}NO (upper series) or ^{15}NO (lower series); 200 ppm C_2H_2; 2.5% O_2; SV: 100 L h^{-1} g^{-1}. Spectra collected every 4 °C.

As a consequence, we suggest that these bands would not correspond to vibrations directly involving a nitrogen atom, at least for vibrations where coupling between several modes is minimal. However, the shift of the bands clearly indicates the presence of a nitrogen atom in the adsorbed intermediate species leading to an indirect perturbation (coupling) of other vibration modes [n(CC) or n(CO) for example]. Then, these bands are attributed to $C_XH_YNO_Z$ (I) species while the exact vibrational assignment remains unclear.

Concerning the band at 1608 cm^{-1}, it presents a lower isotopic shift factor (0.9708) than those reported in Table 2, being however more representative of a n(NO) than a n(CN) mode. A bibliographic survey reveals that when the degenerated n_3 vibrational mode of nitrates species splits, the isotopic shift factor falls between 0.9752 and 0.9791 independently on the nitrate configuration (bidentate, bridged) formed over Cu-zeolites [22]. We thus decide to assign the band at 1608 cm^{-1} (under ^{14}NO conditions) to the n_3 coupled mode of bridged nitrates that shifts to 1561 cm^{-1} under ^{15}NO, even if the isotopic shift factor is lower than those already reported. It is moreover worth nothing that when using ^{15}NO, the band at 1608 cm^{-1} does not completely disappear. This indicates that a nitrogen free carbonaceous species also contributes to this band. Other peaks at 1581, 1378 and 1369 cm^{-1} do not shift under ^{15}NO conditions and correspond to the characteristic bands of formates species. Two kinds of formates species would thus be present as identified by their n_{as} (1608 and 1581 cm^{-1}) and n_S (1378 and 1369 cm^{-1}) vibrations [23]. Finally, regarding the last bands in Fig. 7, those at 1678 and 1700 cm^{-1} are neither shifted when using ^{15}NO. They are assigned to the n(CO) vibrational mode of formaldehyde species (1700 cm^{-1}) and of another intermediate species arising from partial C_2H_2 oxidation (1678 cm^{-1}).

When the temperature increases from 120 to 160 °C (Fig. 8), the formation and shift of bands corresponding to new intermediates species are detected. The isotopic factor for the band at 1634 (^{14}NO) that shifts to 1598 cm^{-1} (^{15}NO) is equal to 0.9778. This value is in agreement with that of NO_2 in the gas phase [24]. These bands are then assigned to NO_2 absorbed onto the catalytic surface after its production from NO oxidation [25].

Similarly to the case of bridged nitrates band (1608 cm^{-1}), the band at 1634 cm^{-1} characterizes simultaneously N containing species (NO_2) and carbonaceous specie since the band at 1634 cm^{-1} is still present under ^{15}NO conditions. It would correspond to a n(C=C) typical for acetylene protonation [16]. Concerning the bands at 1673 and 1677 cm^{-1} that slightly shift to 1663 and 1657 cm^{-1} (more details of these couple of bands on Fig. 9 in the 160–255 °C range), they possess an isotopic shift factor of 0.994, again much higher than those reported in Table 2. Consequently, they cannot characterize 'pure' vibrations involving nitrogen but coupled vibrations such as those present in $H_2C{=}NO$ cannot be ruled out. Based on these results, it is possible to conclude that no n(NO) from organic nitrates (R-ONO) [26–28] nor form nitroso compounds (R-NO) [29] and neither $n_{as}(NO_2)$ from nitro-compounds (R-NO_2) are detected under our acetylene SCR conditions. However, some vibrations related with intermediates species and characterized by two bands at 1673 and 1677 cm^{-1} are sensitive to nitrogen isotopic labelling. These bands thus characterize either a n(CC) or n(CO) vibration perturbed by a neighbouring nitrogen atom. Alternatively, they may characterize a CNO coupled vibration

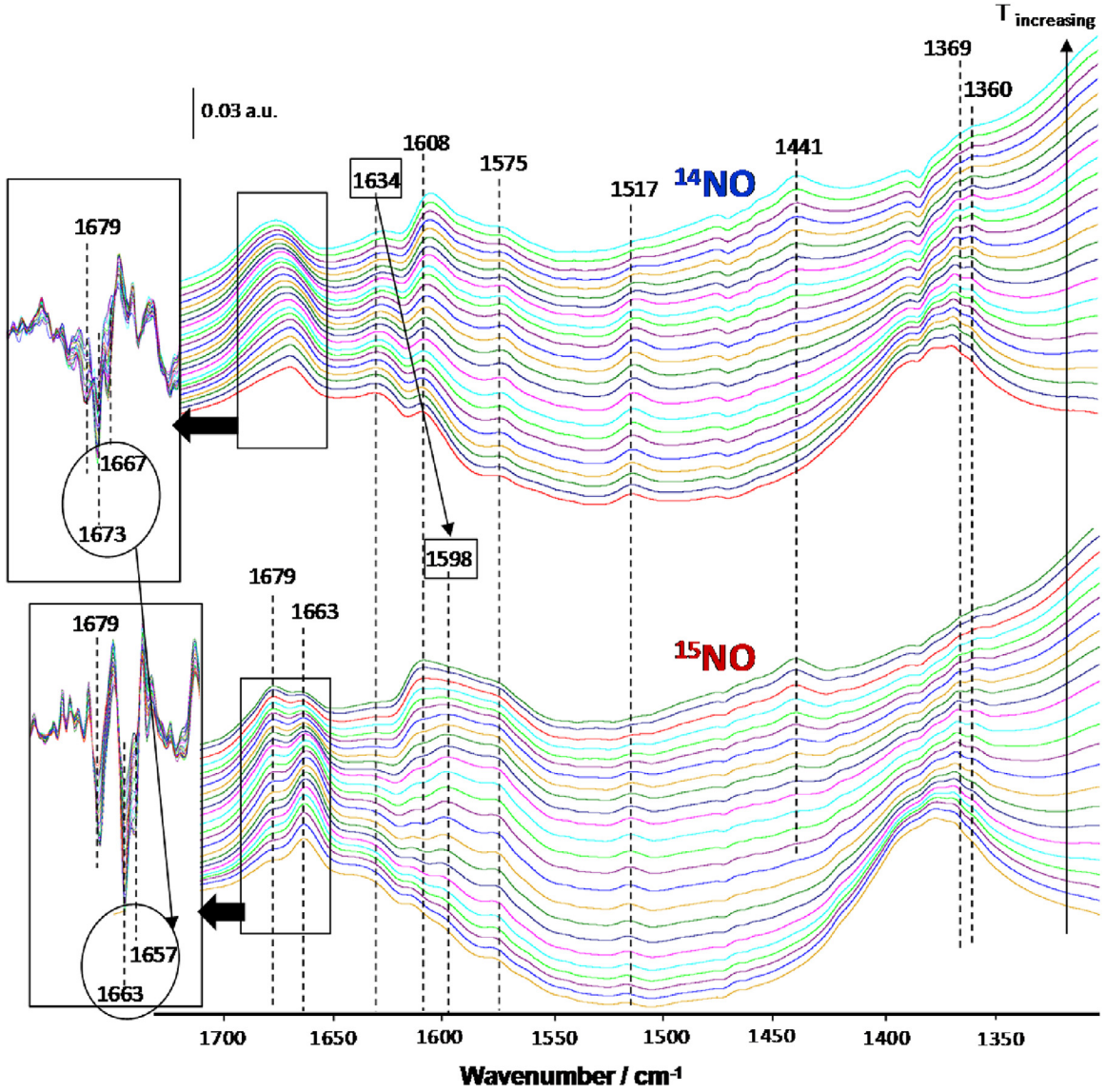

Fig. 9. IR spectra recorded between 160 and 255 °C for 1%Fe–HFER catalyst submitted to NO-SCR catalytic test. Conditions: 400 ppm ^{14}NO (upper series) or ^{15}NO (lower series); 200 ppm C_2H_2; 2.5% O_2; SV: 100 L h^{-1} g^{-1}. Spectra collected every 4 °C.

mode. Following these remarks, it is suggested that another kind of $C_XH_YNO_Z$ (II) intermediates species is formed such as ($H_2C{=}NO$, oxime. . .).

Another interesting infrared region to analyse is the one lying between 2100 and 2250 cm^{-1}. During the ^{14}NO experiment, two couple of bands are observed, the first one at 2210 and 2195 cm^{-1} and the second couple at 2131 and 2120 cm^{-1} (Fig. 10). The wavenumbers of the former are close to that for N_2O in the gas phase [n(NNO) at 2224 cm^{-1}], furthermore the preliminary study adsorption of NO over Cu–HFER showed that N_2O adsorbed at room temperature leads to a pair of bands at 2245 and 2228 cm^{-1}. It seems thus reasonable to assign the couple at 2210 and 2195 cm^{-1} observed in *operando* conditions to N_2O adsorbed on two distinct sites. The latter couple of bands at 2131 and 2120 cm^{-1} could be associated to an adsorbed ketene (CH_2CO): an intermediate product previously detected during a visible light-induced oxidation of C_2H_2 by NO_2. The global equation is $C_2H_2 + NO_2 \rightarrow H_2C{=}C{=}O + NO$ and the formed ketene presents a n(CCO) vibration at 2141 cm^{-1} [30].

On another hand, these two couple of bands are also possibly assigned to isocyanate and cyanide species, respectively, which are among the most important intermediate species in HC-SCR. Fortunately, the isotopic ^{15}NO labelling will allow the discrimination between N_2O or isocyanate species and between ketene or cyanide species. As illustrated in Fig. 10, the whole concerned bands shifts to lower wavenumbers when ^{15}NO is used and thus the hypothesis of ketene formation can be directly rejected. A summary of the observed shifts is presented in Table 3.

Since all the species responsible for these bands correspond to nitrogen-containing species, the further calculation of the isotopic shift factors ($n^i/n_{exp.}$) and the isotopic shifts ($Dn_{exp.}$) is necessary to validate the band assignment. The comparison with reference data leads to the assignment of bands at 2211 and 2193 cm^{-1} to two different isocyanate species (NCO^-) and not to adsorbed N_2O (see Table 3). The values of the corresponding isotopic shift factors are indeed much closer to that of NCO^- (0.993) than that of N_2O (0.969). Finally, the assignment of the couple at 2131-2120 cm^{-1} to two different cyanide species seems also validated by comparing the experimental isotopic shift factor [0.984(5)] with that characteristic for cyanide species [0.9846] already reported [31,32]. However, a preliminary work showed that a n(CH) band at 3224 cm^{-1} evolves

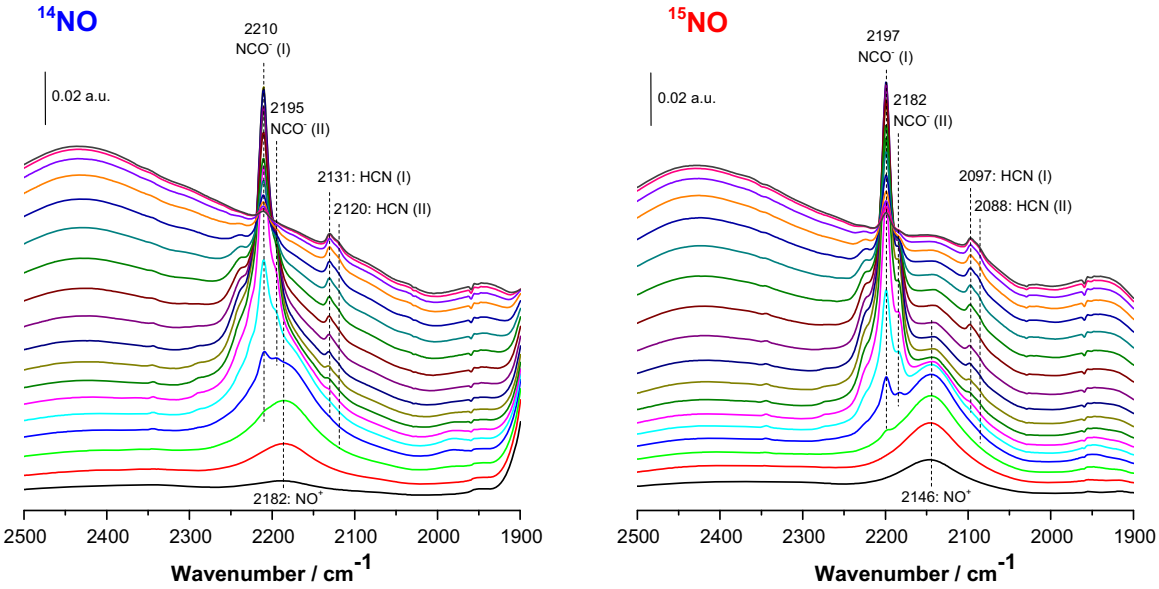

Fig. 10. IR spectra recorded between 104 and 160 °C in the 2000–1900 cm^{-1} region over NO-SCR conditions for the catalytic tests using ^{14}NO or ^{15}NO over Fe–HFER catalyst.

Table 3
A summary of the isotopic effect for cyanides, isocyanate and N_2O species. exp.: experimental; ref.: reference.

Species	Type	$^{14}NO_{exp}$	$^{15}NO_{exp}$	ν_i/ν_{exp}	$\Delta\nu_{exp}$	ν_i/ν_{ref}	Dn_{ref}	References
C≡N	I	2131	2097	0.9841	34	0.9846	33	[31,32]
	II	2120	2088	0.9849	32			
N=C=O	I	2210	2197	0.9941	14	0.993	16	[31,32]
	II	2195	2182	0.9941	13			
N_2O	In gas phase					0.9689	70	[24]

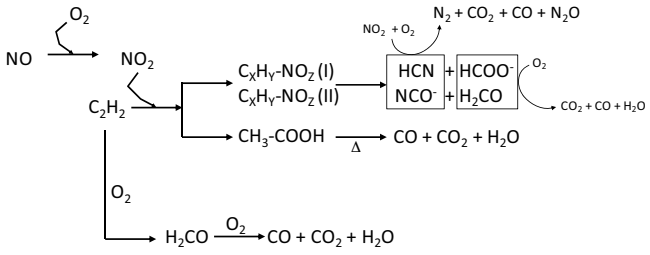

Fig. 11. Reaction mechanism for the NO-SCR by C_2H_2 on 1%Fe–HFER catalyst.

simultaneously with the couple at 2131-2120 cm^{-1} [8] and the assignment to hydrocyanic acid is preferred.

Since the apparition of hydrocyanic acid and isocyanate species is concomitant with the formation of $C_XH_YNO_Z$ (I) and (II) species, the involvement of the later species in SCR is thus strongly suggested. Furthermore, during the *operando* study of the C_2H_2 combustion over Fe–HFER species, bands typical for both adsorbed formaldehyde and formate species were also detected. There simultaneous detection in SCR and C_2H_2 combustion conditions suggests these species as spectator ones for NO_X reduction. Among the two main paths proposed for NO_X removal by HCs [33], the one involving $C_xH_yNO_z$ intermediate species is then preferred to that reporting an interaction between NO_X and $C_xH_yO_z$. A reaction mechanism summarizing the above discussion is proposed in Fig. 11.

4. Conclusions

The preliminary *in-situ* NO adsorption over copper-containing Ferrierite catalyst showed a strong redox character of Cu^{x+} entities when the sample was pre-treated under reducing or oxidizing conditions. Indeed, NO interaction with copper ions leads to the simultaneous identification of Cu^+, Cu^{2+} ($Cu^{2+} - O^{2-} - Cu^{2+}$ possibly) and Cu^{3+} species independently of the pre-treatment, showing the ability of copper cations for the catalytic decomposition of NO.

Moreover, the adsorption of acetylene over M^{X+}–HFER catalysts (M = Fe or Cu) lead to the identification of distinct $n_{as}(CH)$ and n(CC) vibrations relative to C_2H_2 adsorbed over both Brønsted acid sites and redox centres. Concerning the n(CC), this vibration was not detected upon interaction with Fe^{X+} ions. On the contrary, for Cu^{X+} ones, the marked red-shift of the n(CC) wavenumbers compared to the gas phase would be due to a strong p-retrodonation leading in parallel to a Fermi resonance in the $n_{as}(CH)$ region. Finally, the strong affinity between C_2H_2 and copper ions gives rise to thermal stability of the adsorbed species until 200–250 °C compared to iron ions (100–150 °C).

The strong redox character and the marked thermal stability of adsorbed acetylene displayed by 1%Cu–HFER catalyst makes it a priori a suitable catalyst for NO-SCR by C_2H_2. However, when the NO to NO_2 oxidation reaction was carried out, a relevant NO oxidation to NO_2 was only observed over iron-containing sample. As a consequence, the NO_X reduction efficiency was also higher with the Fe–HFER catalyst. The SCR of NOx is thus improved by the presence of NO_2 and the NO oxidation to NO_2 is considered as an essential reaction step when C_2H_2 is used as reducing agent. A reaction mechanism was finally determined over 1%Fe–FER applying the *IR operando* methodology coupled with the use of labelled ^{15}NO iso-

tope. A $C_XH_YNO_Z$ intermediate species distinct form nitroso, nitrito or nitrato species is proposed. This $C_XH_YNO_Z$ species further give rise to hydrocyanic acid and isocyanates species, considered as the most important intermediates species for NO-SCR when C_2H_2 is used as a reducing agent.

Acknowledgement

The financial support provided by UNICAEN is acknowledged.

Appendix A. Supplementary data

Supplementary data associated with this article can be found, in the online version, at http://dx.doi.org/10.1016/j.apcatb.2017.03.052.

References

[1] E.E. Agency, Air Quality in Europe—2016 Report, Publications Office of the European Union, Luxembourg (Denmark), 2016, http://dx.doi.org/10.2800/80982, ISBN 978-92-9213-847-9 ISSN 1977-8449 http://www.eea.europa.eu/publications/air-quality-in-europe-2016.
[2] M. Iwamoto, H. Yahiro, K. Tanda, N. Mizuno, Y. Mine, S. Kagawa, et al., Removal of nitrogen monoxide through a novel catalytic process. 1. Decomposition on excessively copper-ion-exchanged ZSM-5 zeolites, J. Phys. Chem. 95 (1991) 3727–3730, http://dx.doi.org/10.1021/j100162a053.
[3] C. Wang, X. Wang, S. Yu, Y. Xu, Acetylene A new reducing agent used in SCR of NO on zeolite catalysts in a oxygen-rich atmosphere, React. Kinet. Catal. Lett. 86 (2005) 59–66.
[4] X. Wang, H. Yang, Q. Yu, S. Zhang, C2H2-SCR of NO over HZSM-5 affected by intracrystalline diffusion of NOx, Catal. Lett. 113 (2007) 109–114, http://dx.doi.org/10.1007/s10562-007-9014-z.
[5] X. Wang, Y. Xu, S. Yu, C. Wang, The first study of SCR of NOx by acetylene in excess oxygen, Catal. Lett. 103 (2005) 101–108, http://dx.doi.org/10.1007/s10562-005-6509-3.
[6] A. Kubacka, J. Janas, E. Włoch, B. Sulikowski, Selective catalytic reduction of nitric oxide over zeolite catalysts in the presence of hydrocarbons and the excess of oxygen, Catal. Today 101 (2005) 139–145, http://dx.doi.org/10.1016/j.cattod.2005.01.011.
[7] S. Wuttke, P. Bazin, A. Vimont, C. Serre, Y.K. Seo, Y.K. Hwang, et al., Discovering the active sites for C3 separation in MIL-100(Fe) by using operando IR spectroscopy, Chem.-A Eur. J. 18 (2012) 11959–11967, http://dx.doi.org/10.1002/chem.201201006.
[8] I. Castellanos, O. Marie, An operando FT-IR study of the NOx SCR over Co-HFER and Fe-HFER using acetylene as a reducing agent, Catal. Today 283 (2017) 54–65.
[9] E. Ivanova, M. Mihaylov, K. Hadjiivanov, V. Blasin-Aubé, O. Marie, A. Plesniar, et al., Evidencing three distinct FeII sites in Fe–FER zeolites by using CO and NO as complementary IR probes, Appl. Catal. B Environ. 93 (2010) 325–338, http://dx.doi.org/10.1016/j.apcatb.2009.10.006.
[10] V. Blasin-Aube, O. Marie, J. Saussey, A. Plesniar, M. Daturi, N. Nguyen, et al., Iron nitrosyl species in Fe-FER: a complementary Mössbauer and FTIR spectroscopy study, J. Phys. Chem. C 113 (2009) 8387–8393.
[11] S. Bordiga, C. Lamberti, F. Bonino, A. Travert, T.-S. Frédéric, F. Thibault-Starzyk, Probing zeolites by vibrational spectroscopies, Chem. Soc. Rev. 44 (2015) 7262–7341, http://dx.doi.org/10.1039/C5CS00396B.
[12] P. Da Costa, B. Modén, G.D. Meitzner, D.K. Lee, E. Iglesia, Spectroscopic and chemical characterization of active and inactive Cu species in NO decomposition catalysts based on Cu-ZSM5, Phys. Chem. Chem. Phys. 4 (2002) 4590–4601, http://dx.doi.org/10.1039/b203700a.
[13] C. Henriques, NO+ ions as IR probes for the location of OH groups and Na+ ions in main channels and side pockets of mordenite, Microporous Mesoporous Mater. 50 (2001) 167–171, http://dx.doi.org/10.1016/S1387-1811(01)00444-9.
[14] M. Tortorelli, K. Chakarova, L. Lisi, K. Hadjiivanov, Disproportionation of associated Cu2+ sites in Cu-ZSM-5 to Cu+ and Cu3+ and FTIR detection of Cu3+(NO)x (x=1 2) species, J. Catal. 309 (2014) 376–385, http://dx.doi.org/10.1016/j.jcat.2013.10.018.
[15] D. Smith, Studies of silica-supported metal chloride catalysts for the vapor-phase hydrochlorination of acetylene, J. Catal. 11 (1968) 113–130, http://dx.doi.org/10.1016/0021-9517(68)90018-3.
[16] S. Bordiga, G. Ricchiardi, G. Spoto, D. Scarano, L. Carnelli, A. Zecchina, et al., Acetylene, methylacetylene and ethylacetylene polymerization on H-ZSM5: a spectroscopic study, J. Chem. Soc. Faraday Trans. 89 (1993) 1843, http://dx.doi.org/10.1039/ft9938901843.
[17] A. Itadani, T. Yumura, T. Ohkubo, H. Kobayashi, Y. Kuroda, Existence of dual species composed of Cu+ in CuMFI being bridged by C2H2, Phys. Chem. Chem. Phys. 12 (2010) 6455, http://dx.doi.org/10.1039/c000967a.
[18] T. Shimanouchi, Tables of molecular vibrational frequencies: part 6, J. Phys. Chem. Ref. Data 2 (1973) 121–162, http://dx.doi.org/10.1063/1.3253114.
[19] P.S. Cremer, X. Su, Y.R. Shen, G.A. Somorjai, Temperature-dependent rearrangements and reactions of acetylene adsorbed on Pt(111) monitored in the range 125–381 K by sum frequency generation, J. Phys. Chem. B 101 (1997) 6474–6478, http://dx.doi.org/10.1021/jp9705380.
[20] J. Armor, Catalytic reduction of nitrogen oxides with methane in the presence of excess oxygen: a review, Catal. Today 26 (1995) 147–158, http://dx.doi.org/10.1016/0920-5861(95)00134-2.
[21] T. Weingand, S. Kuba, K. Hadjiivanov, H. Knözinger, Nature and reactivity of the surface species formed after NO adsorption and NO + O2 coadsorption on a WO3–ZrO2 catalyst, J. Catal. 209 (2002) 539–546, http://dx.doi.org/10.1006/jcat.2002.3654.
[22] H.Y. Chen, Z. Wei, M. Kollar, F. Gao, Y. Wang, J. Szanyi, et al., NO oxidation on zeolite supported Cu catalysts: formation and reactivity of surface nitrates, Catal. Today 267 (2016) 17–27, http://dx.doi.org/10.1016/j.cattod.2015.11.039.
[23] T. Nobukawa, M. Yoshida, S. Kameoka, S. Ito, K. Tomishige, K. Kunimori, In-Situ observation of reaction intermediate in the selective catalytic reduction of N2O with CH4 over Fe ion-exchanged BEA zeolite catalyst for the elucidation of its reaction mechanism using FTIR, J. Phys. Chem. B 108 (2004) 4071–4079, http://dx.doi.org/10.1021/jp030867u.
[24] S. Pinchas, I. Laulicht, Infrared Spectra of Labelled Compounds, Academic Press, New York, NY, 1971.
[25] M. Iwasaki, H. Shinjoh, NO evolution reaction with NO2 adsorption over Fe/ZSM-5: in situ FT-IR observation and relationships with Fe sites, J. Catal. 273 (2010) 29–38, http://dx.doi.org/10.1016/j.jcat.2010.04.023.
[26] B.I. Mosqueda-Jiménez, A. Jentys, K. Seshan, J.A. Lercher, On the surface reactions during NO reduction with propene and propane on Ni-exchanged mordenite, Appl. Catal. B Environ. 46 (2003) 189–202, http://dx.doi.org/10.1016/S0926-3373(03)00212-1.
[27] Y. Chi, S.S.C. Chuang, Effect of oxygen concentration on the reduction of NO with propylene over CuO/Al2O3, Catal. Today 62 (2000) 303–318, http://dx.doi.org/10.1016/S0920-5861(00)00432-6.
[28] H. He, J. Wang, Q. Feng, Y. Yu, K. Yoshida, Novel Pd promoted Ag/Al2O3 catalyst for the selective reduction of NOx, Appl. Catal. B Environ. 46 (2003) 365–370, http://dx.doi.org/10.1016/S0926-3373(03)00242-X.
[29] E. Pretsch, P. Bühlmann, M. Badertscher, Structure Determination of Organic Compounds, Springer Berlin Heidelberg, Berlin, Heidelberg, 2009, http://dx.doi.org/10.1007/978-3-540-93810-1.
[30] J.A. Harrison, H. Frei, Visible light-induced oxygen transfer from nitrogen dioxide to ethyne and propyne in a cryogenic matrix. 2. mechanism and regioselectivity, J. Phys. Chem. 98 (1994) 12152–12157, http://dx.doi.org/10.1021/j100098a007.
[31] S. Chansai, R. Burch, C. Hardacre, J. Breen, F. Meunier, The use of short time-on-stream in situ spectroscopic transient kinetic isotope techniques to investigate the mechanism of hydrocarbon selective catalytic reduction (HC-SCR) of NOx at low temperatures, J. Catal. 281 (2011) 98–105, http://dx.doi.org/10.1016/j.jcat.2011.04.006.
[32] Y.H. Yeom, B. Wen, W.M.H. Sachtler, E. Weitz, NOx reduction from diesel emissions over a nontransition metal zeolite catalyst: a mechanistic study using FTIR spectroscopy, J. Phys. Chem. B 108 (2004) 5386–5404, http://dx.doi.org/10.1021/jp037504e.
[33] O. Gorce, F. Baudin, C. Thomas, P. Da Costa, G. Djega-Mariadassou, On the role of organic nitrogen-containing species as intermediates in the hydrocarbon-assisted SCR of NOx, Appl. Catal. B Environ. 54 (2004) 69–84, http://dx.doi.org/10.1016/j.apcatb.2004.05.022.